Analytical Methods

PAPER

View Article Online
View Journal | View Issue

Cite this: *Anal. Methods*, 2014, **6**, 4746

Amplified electrochemiluminescence of lucigenin triggered by electrochemically reduced graphene oxide and its sensitive detection of bisphenol A

Hong Dai,*[a] Shupei Zhang,[a] Yanyu Lin,[ab] Yan Ma,[c] Lingshan Gong,[a] Guifang Xu,[a] Mei Fu,[a] Xiuhua Li[a] and Guonan Chen*[b]

Received 26th March 2014
Accepted 3rd May 2014

DOI: 10.1039/c4ay00750f

www.rsc.org/methods

An amplified and stable electrochemiluminescent signal of lucigenin was observed on an electrochemically reduced graphene oxide-containing sensing platform. Herein, chitosan was used as an excellent dispersant, which favors the better dispersion of graphene oxide in solution and improved electrochemical reduction of graphene oxide. The electrochemically reduced graphene oxide showed outstanding conductivity which was propitious to the transfer of electrons, leading to the enhancement of the electrochemiluminescent signals of lucigenin. In addition, bisphenol A, as a classical food borne pollutant, was first detected due to its strong inhibiting action of the electrochemiluminescent response of lucigenin. Then, we studied the quenched electrochemiluminescent system and the possible mechanism of the platform in detail. Under optimum conditions, the proposed electrochemiluminescent sensor exhibited a linear response range from 1.0×10^{-9} mol L^{-1} to 1.0×10^{-4} mol L^{-1} with a low detection limit of 3.0×10^{-10} mol L^{-1} for bisphenol A, which might find promising applications in developing a new type of biosensor.

Published on 06 May 2014. Downloaded by Duke University on 25/04/2018 22:20:45.

1 Introduction

In electrochemiluminescence, also known as electrogenerated chemiluminescence, electric energy is converted into light energy at the electrode surface through an applied potential.[1,2] Luminescent signals can be obtained from the excited states of an electrochemiluminescent (ECL) luminophore generated at electrode surfaces during an electrochemical reaction.[1,2] In recent years, there has been a steady growth of focus on electrochemiluminescence, which is considered as an important and valuable detection method in analytical chemistry due to its high sensitivity, high selectivity and good reproducibility.[3,4] Furthermore, ECL sensors not only retain the advantages of chemiluminescence (CL) sensors, such as excellent sensitivity and a wide dynamic concentration response range, but also have some additional advantages over the CL sensors.[3,4] Consequently, much research has been done on three ECL compounds, which include lucigenin (*N*,*N*-dimethyl-9,9-biacridinium dinitrate), luminol and ruthenium complexes, particularly tris(2,2′-bipyridine)ruthenium(II) ($Ru(bpy)_3^{2+}$).[1,5] We found that, compared with the ECL reagents of luminol and $Ru(bpy)_3^{2+}$, there are only a few studies regarding the ECL of lucigenin in aqueous media and analytical applications owing to bad reproducibility. Takeo Ohsaka and Takeyoshi Okajima discovered that the sensitivity and reproducibility of the ECL of lucigenin can be improved when doing some research on the modified electrode with self-assembled monolayers and on solutions with surfactants.[6] Therefore, extending analytical applications of lucigenin to find a new method for solving the problem of insoluble electrochemical luminescence absorption on the surface of electrode is of great importance.

In recent years, tremendous attention has been paid to graphene together with its various derivatives,[7] such as reduced graphene oxide (RGO),[8,9] graphene nanoribbon[10] and nitrogen-doped graphene,[11] because of their excellent electrical conductivity. In particular, RGO, a two-dimensional material, is robust and popular because of its good dispersibility, convenient chemical modification, good mechanical and thermal properties, high surface area, easy functionalization and good biocompatibility.[12] These interesting properties make RGO a promising material for extraordinary applications in various fields such as batteries,[13] catalysis,[14] nanoelectronics[15] and supercapacitors.[16] Various methods, such as micromechanical cleavage,[17] solvothermal synthesis,[18] epitaxial growth[19,20] and liquid-phase exfoliation,[21–23] have been proposed to prepare RGO. However, the widespread applications of RGO are limited by high temperature, special equipment and conditions, and tedious procedures during its preparation. Recently, it has been reported that graphene sheets can be prepared using GO as a

---

[a] *College of Chemistry and Chemical Engineering, Fujian Normal University, Fuzhou, Fujian, 350108, China. E-mail: dhong@fjnu.edu.cn; gnchen@fzu.edu.cn; Fax: +86-591-22866135*

[b] *Ministry of Education Key Laboratory of Analysis and Detection for Food Safety, Fujian Provincial Key Laboratory of Analysis and Detection for Food Safety, Fuzhou University, Fuzhou, Fujian, 350002, China*

[c] *Fuzhou Entry-Exit Inspection & Quarantine Bureau of P.R.C, Fuzhou, Fujian, 350002, China*

This journal is © The Royal Society of Chemistry 2014

Published on 06 May 2014. Downloaded by Duke University on 25/04/2018 22:20:45.

precursor in bulk by the non-composite conversion of GO into "chemically reduced" graphene oxide making use of thermal treatment[24] or chemical reducing agents,[25] which may be cheap and of high synthesizing efficiency but are poisonous and intricate. More recently, Srinivasan Sampath has successfully combined Raman spectroscopy with electrochemistry to accomplish the electrochemical reduction of GO to RGO, and realized an *in situ* Raman spectroelectrochemical study.[26] Shaojun Dong actualized the controlled synthesis of large-area and patterned electrochemically reduced graphene oxide (ERGO) films.[27] Direct electrochemical reduction of single-layer GO and subsequent functionalization with glucose oxidase have been achieved by Hua Zhang and coworkers,[28] which resulted in more highly conducting graphene that possessed better biocompatibility with electrode materials. Therefore, it is in our interest to develop an efficient, facile, environmentally friendly and low-cost electrochemical method to produce RGO films. Herein, we dispersed GO in a certain concentration of chitosan (CS) solution and cast this GO–CS solution on the bare gold electrode, then reduced the modified electrode at a certain potential. Not only did this modified electrode amplify the ECL emission of lucigenin, but it also evidently improved the stability of the ECL response of lucigenin. Herein, CS was used to disperse GO and provide an excellent environment to construct sensors due to its attractive properties, including excellent high permeability toward water, film-forming ability, biocompatibility, good adhesion, nontoxicity, biocompatibility, high mechanical strength and a susceptibility to chemical modifications.[29–32] Besides, an ECL inhibition method for the determination of trace bisphenol A (BPA) has been established based on the strong inhibition phenomenon of BPA to the ECL values of lucigenin. Under the optimum conditions, the sensor exhibited high sensitivity, good stability and specificity for the quantitative detection of BPA, which may have promising applications for the fabrication of ECL array sensors.

2 Experimental

2.1 Reagents

Chitosan (CS), potassium ferricyanide [$K_3Fe(CN)_6$], potassium ferrocyanide [$K_4Fe(CN)_6$], potassium chloride (KCl), hydrochloric acid (HCl), acetic acid (CH_3COOH) and sodium acetate (CH_3COONa) were purchased from Chemicals Co., Ltd. (Shanghai, China). 0.1 mol L^{-1} acetate buffer solutions at various pH values were prepared from stock solutions of 0.1 mol L^{-1} CH_3COOH and CH_3COONa. Lucigenin was obtained from Fluka Chemie AG. A 1.0×10^{-3} mol L^{-1} stock solution of lucigenin was prepared by dissolving lucigenin in redistilled water. All the reagents were used without further purification. All the aqueous solutions and water for rinsing were prepared from ultrapure water from a Milli-Q plus system (Millipore Co., > 18 MΩ cm).

2.2 Apparatus

A homemade ECL system, including a BPCL Ultra-Weak Chemiluminescence Analyzer (Institute of Biophysics, Chinese Academy of Sciences) for detecting light emission and an Electrochemistry Working Station (Chenhua 660A, Shanghai, China), was used to detect ECL intensity *versus* potential. All the experiments were carried out with a conventional three-electrode system in which a gold electrode (GE) (2 mm diameter), KCl-saturated silver–silver chloride (Ag/AgCl) and a platinum wire acted as the working, reference and counter electrodes, respectively. All the potentials reported here refer to the Ag/AgCl (sat. KCl) reference electrode. X-ray photoelectron spectroscopy (XPS) measurements were carried out with an ESCALAB 250 Å 1314. Transmission Electron Microscope (TEM) measurements were executed with a JEM-2100F, Janpan. pH of the solutions were measured on a pHS-3C pH meter equipped with a composite pH glass electrode (Shanghai Dapu Instr. Inc., China), after careful pH calibrations.

2.3 Preparation of GO–CS colloidal suspensions

The preparation of GO was based on the Hummers' method described in the literature.[33] In a typical procedure, 0.2 g of graphite powder was added into 3.5 mL H_2SO_4 and stirred for 2 h, simultaneously, 0.6 g of $KMnO_4$ was slowly added to maintain the temperature of the solution below 293 K under constant stirring. The resulting mixture was then stirred at 308 K for 30 min, and then 15 mL H_2O and 2 mL 30% H_2O_2 solutions were added to terminate the oxidation. Then, the mixture was repeatedly washed with 5% HCl aqueous solution until the pH became neutral. 16 mL water was added into the resulting precipitate and sonicated well to obtain GO. The brown dispersion was centrifuged at 4000 rpm for 2 h to remove any unexfoliated GO. Then, 8 mg mL^{-1} of GO suspension was prepared by dissolving 4 mg GO in 500 μL deionized water and vibrating for 5 min at room temperature until a homogeneous GO solution was obtained. A 1.0% CS solution was prepared by dissolving 1.0 g CS solid in 100 mL 1.0% acetic acid solution and stirring for several hours at room temperature until reaching a homogeneous CS solution. The CS solution was stored in a refrigerator when it was not in use. A certain proportion of GO–CS was prepared by mixing a certain volume of 8 mg mL^{-1} GO suspensions with a certain volume of 1.0% chitosan solution, and then vibrating and sonicating until a homogeneous solution was obtained.

2.4 Preparation and reduction of GO–CS modified gold electrode

The mechanism of the fabrication of the ECL sensor is shown in Scheme 1A. Before modification, the bare gold electrode (GE) was first polished with 0.05 μm alumina slurry, sonicated in deionized water to remove any traces remaining, immersed in freshly prepared Piranha solution 30% H_2O_2 and concentrated H_2SO_4, 3 : 1 (v/v) for 10 min, and finally electrochemically pretreated by cyclic potential scanning between 1.4 V and −0.2 V in 0.1 mol L^{-1} H_2SO_4 until a cyclic voltammogram of a clean gold electrode was obtained. During modification, 3 μL of prepared GO–CS colloidal suspension was casted on the pre-treated gold electrode, dried under infrared lamp and cooled to room temperature. Then, the GO–CS modified gold electrode was

Published on 06 May 2014. Downloaded by Duke University on 25/04/2018 22:20:45.

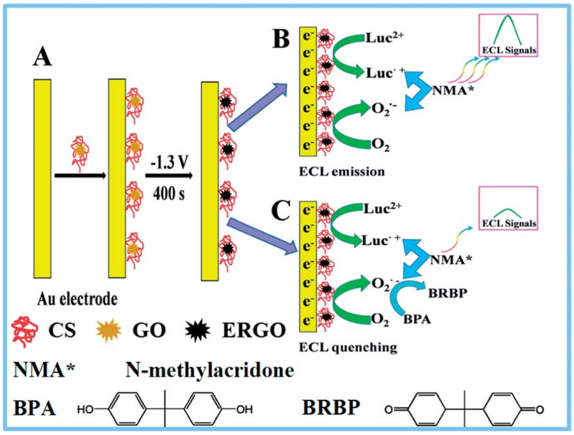

Scheme 1 Schematic representation of (A) the preparation of the ERGO–CS modified electrode, (B) the mechanism of ECL emission of lucigenin and (C) the possible mechanism for quenching of ECL by BPA.

reduced in $CH_3COOH–CH_3COONa$ (pH 5.0) buffer with 0.1 mol L^{-1} KCl solution at −1.3 V for 400 s.

3 Results and discussion

3.1 The morphology of the reduced modified electrode

The morphological and structural characterization of GO was performed by TEM. As shown in Fig. 1A, we clearly found that GO possessed a transparent and large layered structure, similar to a silk veil. The XPS of the GO–CS and ERGO–CS modified gold electrodes are exhibited in Fig. 1B and C, respectively. The peaks at 284.5, 286.4 and 288.2 eV represent the C–C, C–O and C═O bands in graphene-based materials, respectively. By comparing Fig. 1B with C, after electrochemical reduction, we can see that the peak intensity of functional groups that contain oxygen decreased tremendously while that of the carbon–carbon bond increased. The results confirmed the effectiveness of electrochemical reduction and that GO can be reduced by the electrochemical method in the CS modified layer.

3.2 Electrochemical behavior of various modified electrodes

Cyclic voltammograms (CVs) of ERGO–CS/GE (a), GO–CS/GE (c) and GE (b) can be seen in Fig. 2A. A classic pair of redox peaks was obtained at the bare gold electrode. Whereas, the introduction of the GO/CS composite film significantly dwindled the oxidation/reduction of $Fe(CN)_6{}^{3-/4-}$ on the electrode, which was because of not only GO acting as an insulator impeding the transfer of electron in the electrode surface, but also the electrostatic repulsion between GO/CS composite and electrochemical probes. It is especially noteworthy that we found the value of the peak current of the reduced modified electrode at −1.3 V for 400 s to be bigger than that of the bare gold electrode. This is mainly due to the electrochemical reduction of ERGO possessing high conductivity, which would lead to electron transfer in the electrode surface and the reduction of negative charge in the ERGO–CS membrane which reduced the electrostatic repulsion to $Fe(CN)_6{}^{3-}$. The result was consistent with the phenomenon reported in early reports, such as Navarro[9] who observed a three-order increase in conductivity when GO was chemically reduced using hydrazine to RGO. Hua Zhang[28] found that the redox peak of RGO–CS modified gold electrode in $[Fe(CN)_6]^{3-/4-}$ was almost the same as that of the bare GCE, which also indicated that the conductivity of the electrochemical RGO was as good as that of GCE.

Fig. 2B showed the CVs of the modified electrodes in $K_3[Fe(CN)_6]$ solution with various potential scan rates. The relationship between redox peak current of $[Fe(CN)_6]^{3-/4-}$ and the square root of the scan rate were used to assess the properties of the electrode, described by the following Randles–Sevcik equation:[34]

$$i_p = (2.69 \times 105) n^{3/2} A D^{1/2} C_0 v^{1/2}$$

From Fig. 2B inset, we can conclude that the anodic and cathodic peak currents varied linearly with the square root of the scan rate, suggesting that the reaction was a diffuse-controlled process.

The Randles circuit was selected to obtain the impedance data. As we all know, the resistance to charge transfer (R_{ct}) and the diffusion impedance (W) were both parallel to the interfacial capacitance (C_{dl}). The diameter of the semicircle changed corresponding to the interfacial electron-transfer resistance (R_{ct}). From Fig. 2C, we could easily find that the diameter of the semicircle of the bare gold electrode was the smallest, and that of the ERGO–CS modified electrode was much smaller than the GO–CS modified electrode. We can learn from the phenomenon

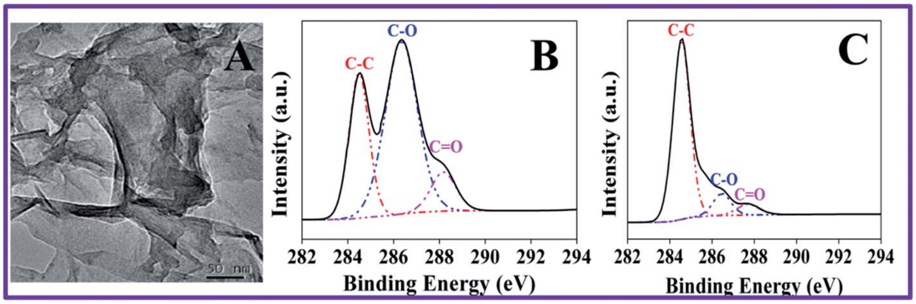

Fig. 1 (A) TEM image of GO in CS solution, XPS images of the GO–CS (B) and REGO–CS (C) modified electrodes.

This journal is © The Royal Society of Chemistry 2014

Published on 06 May 2014. Downloaded by Duke University on 25/04/2018 22:20:45.

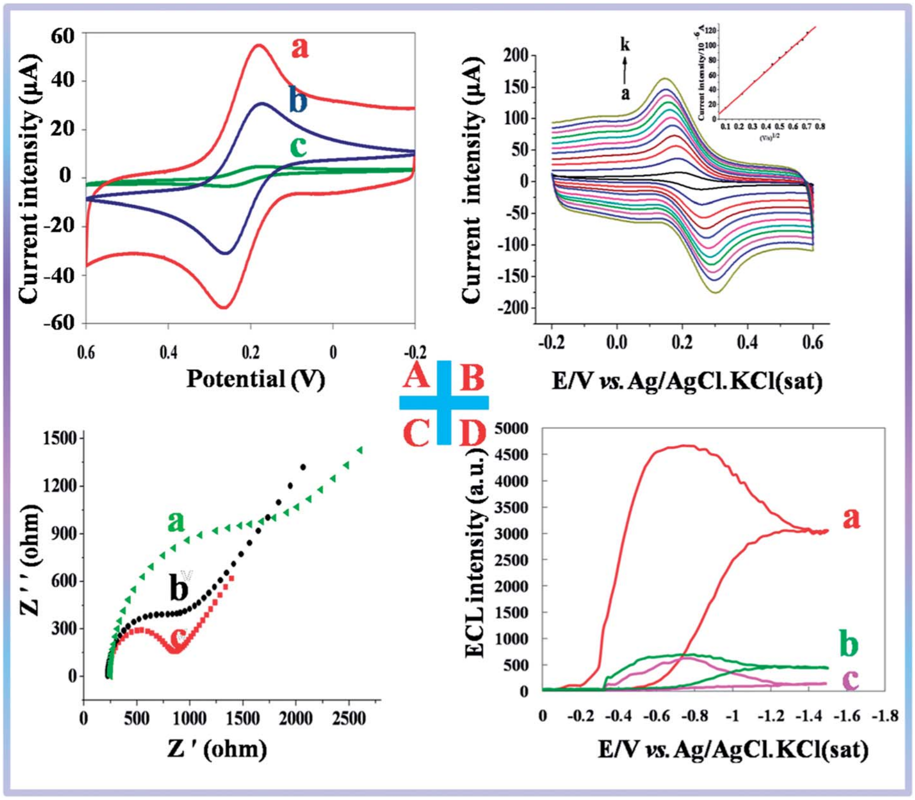

Fig. 2 (A) Cyclic voltammograms of REGO–CS modified electrode (a), bare gold electrode (b), and the GO–CS modified gold electrode (c) in 5 mmol L^{-1} $[Fe(CN)_6]^{3-}$ solution containing 0.3 mol L^{-1} KCl, scan rate: 0.1 V s^{-1}; (B) cyclic voltammograms of reduced GO–CS modified electrode in 5 mM $K_3[Fe(CN)_6]$ solution containing 0.3 M KCl with different scan rates and the linear relationship between the peak currents and the square root of the scan rates (the inset in B), scan rate (a–k) is from 500 to 10 mV s^{-1}; (C) Nyquist plots of (a) GO–CS modified, (b) ERGO–CS modified, and (c) bare gold electrodes in 5 mmol L^{-1} $[Fe(CN)_6]^{3-}$ solution containing 0.01 mol L^{-1} KCl, frequency range: 0.1 to 10 KHz; (D) the ECL of different electrodes in 0.1 mmol L^{-1} KCl containing 20 μmol L^{-1} lucigenin with a scan rate of 0.1 V s^{-1}, (a) ERGO–CS modified gold electrode, (b) bare gold electrode, (c) GO–CS modified gold electrode.

that the conductivity of the reduced electrode was better than the unreduced one, and that the ERGO–CS composite film could function as an efficient electron conducting tunnel between the electrode and the electrolyte.

3.3 ECL characteristics of various modified electrodes

We can see from Fig. 2D that the ECL values at the bare gold electrode and GO–CS/GE were very low. However, the ECL values of ERGO–CS/GE increased to 4500, almost nine-fold compared with that of GO–CS/GE, demonstrating that ERGO–CS/GE had a better conductivity. In addition, the electrochemiluminescence of lucigenin on ERGO–CS/GE occurred at a more positive initial voltage, indicating that the ECL process can be carried out faster and easier. From the electrochemical behavior characterization of different modified films, we have found that the electrochemical reduction of GO generated ERGO has good conductivity and it could promote the transfer rate of electrons in the ECL process, which leads to faster and stronger ECL intensity. Simultaneously, negatively charged chitosan was propitious to positively charged lucigenin absorbed on the electrode surface by electrostatic attraction, which lead to the ECL intensity enhancement of lucigenin in the ERGO–CS composite film modified gold electrode.

The ECL mechanism of lucigenin at −0.6 V has been studied and can be seen in Scheme 1B. Primarily, electrons were transferred from the electrode to lucigenin and O_2 through ERGO–CS, which lead to the generation of Luc^{+} and $O_2^{\bullet-}$. Herein, the cathodic ECL originated from the formation of excited-state NMA* *via* the transformation of dioxetane, which was generated by the reaction of $Luc^{\bullet+}$ and $O_2^{\bullet-}$.[35–39] The corresponding ECL mechanism could be formulated as follows:

$$Luc^{2+} + e^- \rightarrow Luc^{\bullet+} \tag{1}$$

$$O_2 + e^- \rightarrow O_2^{\bullet-} \tag{2}$$

$$Luc^{\bullet+} + O_2^{\bullet-} \rightarrow \text{dioxetane} \rightarrow NMA + NMA^* \tag{3}$$

$$NMA^* \rightarrow NMA + h\nu \tag{4}$$

3.4 Factors influencing ECL emission on ERGO–CS/GE

The parameters of the modified electrode affected not only the ECL intensity but also the reproducibility of the proposed ECL method. Thus, we chose some parameters to investigate to get the best analytical performance.

Published on 06 May 2014. Downloaded by Duke University on 25/04/2018 22:20:45.

3.4.1 Effect of GO concentration. From Fig. 3A we can see that the ECL intensity first increased and then decreased with an increase in the concentrations of GO, and the maximum response was obtained at a concentration of 1.5 mg mL^{-1}, which was attributed to the EGRO obtained by the process of electrochemically reducing the GO being helpful for the electron transfer. Besides, the increased surface area of the electrode supported substance transportation and contributed to the enhancement of the ECL intensity. However, when the concentration was higher than 1.5 mg mL^{-1}, the thicker modified membrane hindered the mass transfer of reactants resulting in a decrease in ECL intensity.[40] Therefore, 1.5 mg mL^{-1} GO was selected as an optimal concentration for this electrochemical sensor.

3.4.2 Reduction potential effect. As shown in Fig. 3B, only weak ECL signals could be found when the reduction potential was lower than −1.0 V, which may be because of the trace amounts of ERGO. Moreover, we found that in a certain range, the higher the reduction potential, the higher will be the ECL intensity. The ECL intensity will remain steady after −1.3 V, suggesting that the GO in the composite film could be almost reduced at −1.3 V.

3.4.3 Reduction time dependence. The reduction time clearly influenced the ECL signals. When the duration was less than 400 s, the ECL intensity increased with the reduction time and then reached the highest at 400 s. Over 400 s, the ECL value decreased quickly, as can be seen in Fig. 3C. This may be due to the electrode surface performance clustering sharply, which was harmful for the electron delivery. The construction of CS would be violated when reduction time was longer than 400 s at the optimal potential.

3.4.4 The influence of dispensed volume. As can be seen from Fig. 3D, the highest ECL intensity was obtained when the dispensed volume was 3 μL. The possible reason was that too much modified volume was unfavorable for ECL behavior and resulted in an increase of non-conductive GO, resulting in weaker electron conduction. The thick membrane would hinder the mass transfer of reactants.[36]

3.4.5 CS concentration dependence. From Fig. 3E we can see that the concentration of CS used for the modified gold electrode had a great influence on the ECL intensity. First, the possible reason could be that the higher the concentration of the CS, the better the dispersion of GO in solution, and the easier it is for the solution to form a membrane, favoring mass transfer. Second, negatively charged CS was propitious to the accumulation of lucigenin on the surface of electrode, which could also lead to an increase in ECL intensity. We tried different concentrations of CS and found that when the value was 0.3%, the ECL was the strongest, thus 0.3% CS was selected for subsequent studies.

3.5 The linearity of lucigenin on the ERGO–CS/GE and GE

Fig. 4A reveals that the linear range of lucigenin on the ERGO–CS/GE is wider than that on the bare gold electrode, ranging from 1.0×10^{-7} mol L^{-1} to 1.0×10^{-4} mol L^{-1}. The regression equation on the ERGO–CS/GE was $\lg(\mathrm{ECL}) = 0.5174 \lg C + 6.0585$ ($R^2 = 0.994$), where ECL is the ECL intensity; C is the concentration of lucigenin. The linear range for lucigenin on the bare gold electrode only ranged from 5.0×10^{-6} mol L^{-1} to 1.0×10^{-4} mol L^{-1}, and the regression equation was $\lg(\mathrm{ECL}) = 1.2918 \lg C + 8.6151$ ($R^2 = 0.997$), where the ECL and C remained the same.

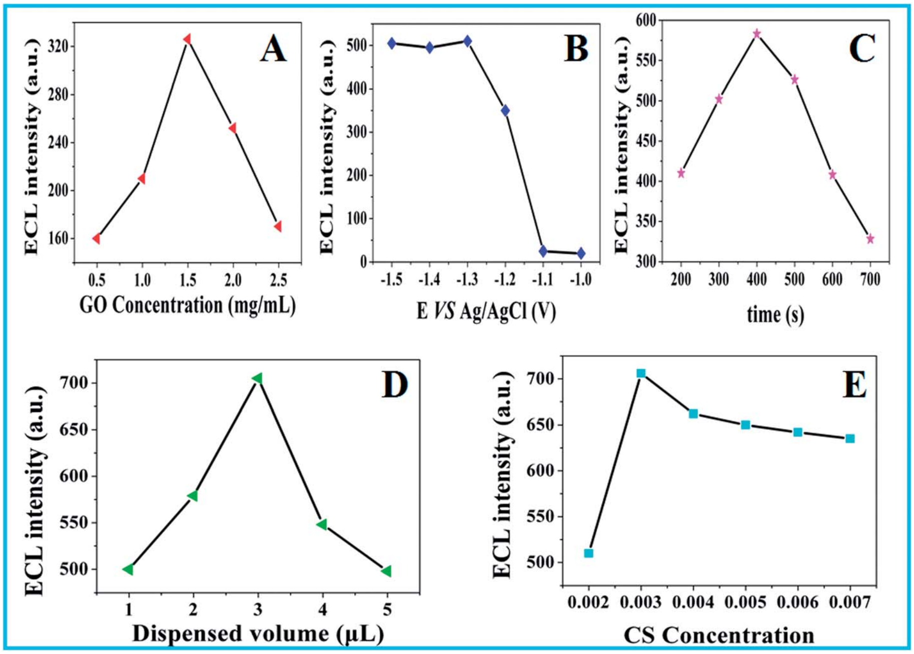

Fig. 3 Effects of (A) the concentration of GO, (B) reduction potential, (C) reduction time, (D) dispensed volume, and (E) the concentration of CS on the ECL intensity of ERGO–CS modified electrode in 0.01 mol L^{-1} KCl containing 20 μmol L^{-1} lucigenin.

Published on 06 May 2014. Downloaded by Duke University on 25/04/2018 22:20:45.

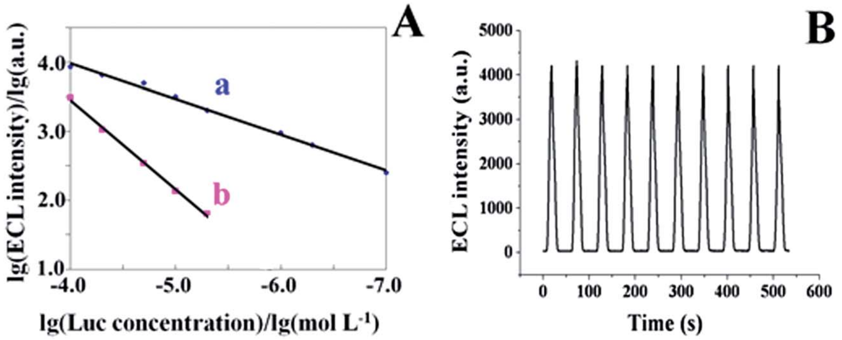

Fig. 4 (A) Calibration plots of lucigenin at (a) ERGO–CS modified gold electrode and (b) bare gold electrode, condition: KCl 0.1 mmol L^{-1} KCl. Potential window: −1.5 to 0 V, scan rate: 0.1 V s^{-1}; (B) ECL signals for duplicate measurements of lucigenin at a concentration of 20 μmol L^{-1} in 0.1 mmol L^{-1} KCl on ERGO–CS modified electrode with a scan rate of 0.1 V s^{-1}.

3.6 Stability and reproducibility of the modified electrode

Fig. 4B showed the ECL intensity of ERGO–CS/GE in the optimal parameters. We can see from the figure that the ECL intensity remained almost the same under the optimum conditions scanning for 10 cycles and the relative standard deviation (RSD) of the ECL intensity was only 5%, which indicated that the prepared sensor possessed good stability and showed potential for practical applications. Reproducibility of the modified electrode was investigated in 20 μmol L^{-1} lucigenin for three different ERGO–CS modified electrodes. Three measurements resulted in a relative standard derivation of 3.4%, showing a good reproducibility of the fabrication protocol. Besides, when the electrode was not in use, it was stored in the shade at room temperature and measured every week. No obvious decrease in the photocurrent response to lucigenin was observed after 2 weeks and 93% of the initial photocurrent response was maintained after one month. This was attributed to the improved hydrophobicity of the membrane on the modified electrode, which played a role in avoiding the absorption of the product of the lucigenin reaction which is hydrophobic. We can take advantage of the stability of the ECL sensor and the stable chemical properties of ERGO in the following studies.

3.7 Practical detection

BPA, an estrogenic endocrine-disrupting chemical, is used in the lacquer lining of metal food cans and water pipes, food packaging and dental sealants, and has been attracting more and more attention due to a large body of reports pointing out that BPA can induce a variety of adverse effects such as abnormal weight gain, prostate cancer and insulin resistance in human. Recently, analysis of BPA has mainly been accomplished by high performance liquid chromatography-mass spectrometry,[41] gas chromatography-mass spectrometry,[42] and liquid chromatography[43] with various detectors. Nonetheless, they are of low sensitivity, time consuming, and need troublesome sample preparation, highly qualified technicians and sophisticated equipment.[44] Consequently, an eco-friendly, fast and sensitive method was developed based on the strong inhibition phenomenon of BPA to the ECL values of lucigenin to monitor trace levels of BPA in biological and environmental samples.

3.7.1 Determination mechanism. Scheme 1C demonstrates the possible mechanism of how the ECL signal of lucigenin is quenched by BPA. The possible quenching mechanism between lucigenin and BPA is similar to that between lucigenin, carbolic acid[37] and aniline.[45] A chemical compound with an electron-donating group, especially $^{\bullet}OH$ or $^{\bullet}NH_2$, would restrain the ECL of lucigenin, while compounds that have intense reduction ability, such as phenol compounds, can act as good antioxidants which could strongly quench the ECL of lucigenin as well. From Fig. 1 we can clearly see that BPA possesses two ·OH. BPA may be oxidized when $O_2^{\bullet-}$ encounters it and thus the chance of $O_2^{\bullet-}$ encountering $Luc^{\bullet+}$ would be reduced simultaneously. Therefore, the ECL values decreased after BPA was injected into the lucigenin solution.

3.7.2 Optimization of conditions for BPA detection. We could see that the ECL intensity was the strongest when the pH was 5.0, as shown in Fig. 5A. This may be ascribed to protonation being involved in the electrochemical reduction process at lower pH values;[37] however, when the pH value was lower than 5.0, the ECL intensity decreased, which could be attributed to the CS and GO being able to dissolve in such a buffer as we all know that the CS could dissolve in acidic solution. Therefore, the ECL detection was performed in buffer solutions of pH 5.0.

Besides, the effect of KCl concentration in buffer solution (5.0) on the ECL intensity of the sensor was investigated, which clearly revealed that the concentration of KCl in buffer solution tremendously influenced the ECL intensity; the lower the lg (concentration of KCl), the stronger the ECL intensity in a certain range. As clearly depicted in Fig. 5B, when the concentration of KCl was higher than 0.01 mol L^{-1}, the background signal increased significantly.[37] The maximum ECL was obtained in 1×10^{-4} mol L^{-1} according to the figure, and when the concentration of KCl was lower than 1×10^{-4} mol L^{-1}, the tendency changed inconspicuously, thus 1×10^{-4} mol L^{-1} was the optimum concentration of KCl.

Finally, the concentration of lucigenin also had a significant influence on the ECL intensity. According to an earlier study, we know that, first, when the concentration was higher than 1×10^{-4} mol L^{-1}, the ECL background signal of lucigenin was quite

Published on 06 May 2014. Downloaded by Duke University on 25/04/2018 22:20:45.

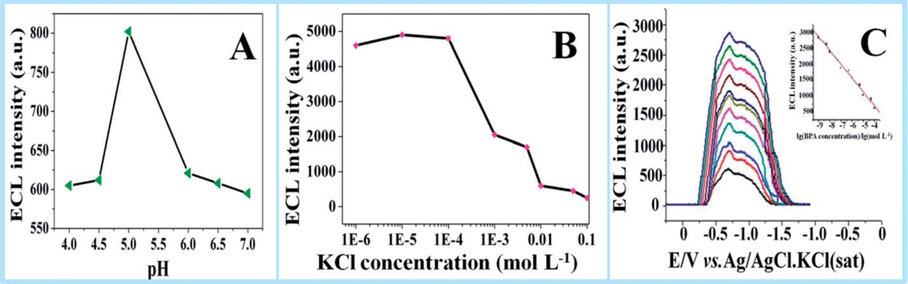

Fig. 5 Effects of pH (A) and KCl concentration (B) on the lucigenin ECL intensity. Conditions: GO 1.5 mg ml^{-1} with 0.3% CS, reduction potential −1.3 V, reduction time 400 s, dispensed volume 3 μL; (C) ECL responses of the proposed sensor to different concentrations (inner to outer is from 1×10^{-4} to 1×10^{-9} mol L^{-1}) of BPA, and linear plot for BPA determination (the inset in C).

high and it weakened the ECL intensity, which was detrimental for achieving higher sensitivity. Second, higher concentrations of lucigenin would produce more reductive product, which was of low solubility and would adsorb on the surface of the modified electrode. Third, lucigenin was expensive. Considering all the above, we selected 1×10^{-4} mol L^{-1} as the optimal concentration of lucigenin.

3.7.3 Calibration curve, linear range and detection limit. As shown in Fig. 5C, as optimum conditions, the ECL intensity was inversely proportional to the concentration of BPA, ranging from 1.0×10^{-9} to 1.0×10^{-4} mol L^{-1}, and the regression equation was $\lg(\mathrm{ECL}) = -423.94 \lg C - 944.2$ ($R^2 = 0.9975$), where ECL is the ECL intensity and C is the concentration of BPA. The relative standard deviation for 1.0×10^{-9} mol L^{-1} BPA was 3.29% ($n = 5$). The detection limit (defined as the concentration that could be detected at a signal-to-noise ratio of 3) was 3×10^{-10} mol L^{-1}.

3.7.4 Interference. The practical utility of a sensor often depends upon its selectivity; thus, the influence of some potential coexisting ions and other compounds in biological samples was investigated. The responses of 500-fold for Na^+, SO_4^{2-}, NO_3^-, 5-fold for maltose, citric acid, sucrose, and 3-fold for uric acid and ascorbic acid had no evident influence on the determination of BPA, suggesting that the novel ECL sensor had high selectivity towards BPA in the presence of other coexisting species.

4 Conclusion

A simple, low cost and high efficiency electrochemical method was used to successfully transform GO into ERGO. A composite film made of GO and CS was used to fabricate a modified gold electrode, and then conventional cyclic voltammetry was posed on the modified electrode to produce an ERGO–CS composite film modified electrode. The proposed new ECL sensor displayed supersensitive and selective detection of BPA through a lucigenin ECL signal amplification mechanism. Due to ERGO possessing better conductivity than GO, it played a significant role in this platform, whereby it greatly avoided the adsorption of electrochemical reaction products on the electrode and greatly improved the sensitivity for detecting BPA. Furthermore, this material could also be used in other areas such as electrochemistry, immunoassay, *etc.* Accordingly, this text presents an important strategy to design ECL sensors and expand their applications for ultratrace amount environmental sensing.

Acknowledgements

This project was financially supported by the NSFC (21205016), National Science Foundation of Fujian Province (2011J05020), Education Department of Fujian Province (JA11062, JB13008, JA13068), Foundation of Fuzhou Science and Technology Bureau (2013-S-113), Fujian normal university outstanding young teacher research fund projects (fjsdjk2012068) was also greatly acknowledged.

References

1 M. M. Richter, *Chem. Rev.*, 2004, **104**, 3003–3036.
2 L. Z. Hu and G. B. Xu, *Chem. Soc. Rev.*, 2010, **39**, 3275–3304.
3 D. Lincot, *Thin Solid Films*, 2005, **487**, 40–48.
4 G. F. Jie, B. Liu, H. C. Pan, J. J. Zhu and H. Y. Chen, *Anal. Chem.*, 2007, **79**, 5574–5581.
5 W. J. Miao, *Chem. Rev.*, 2008, **108**, 2506–2553.
6 T. Okajima and T. Ohsaka, *J. Electroanal. Chem.*, 2002, **534**, 181–187.
7 X. S. Li, W. W. Cai, J. An, S. Kim, J. Nah, D. X. Yang, R. Piner, A. Velamakanni, I. Jung, E. Tutuc, S. K. Banerjee, L. Colombo and R. S. Ruoff, *Science*, 2009, **324**, 1312–1314.
8 G. Eda, G. Fanchini and M. Chhowalla, *Nat. Nanotechnol.*, 2008, **3**, 270–274.
9 C. G. Navarro, R. T. Weitz, A. M. Bittner, M. Scolari, A. Mews, M. Burghard and K. Kern, *Nano Lett.*, 2007, **7**, 3499–3503.
10 X. Li, X. Wang, L. Zhang, S. Lee and H. Dai, *Science*, 2008, **319**, 1229–1232.
11 L. T. Qu, Y. Liu, J. B. Baek and L. M. Dai, *ACS Nano*, 2010, **4**, 1321–1326.
12 J. T. Robinson, S. M. Tabakman, Y. Liang, H. Wang, H. Sanchez Casalongue, D. Vinh and H. Dai, *J. Am. Chem. Soc.*, 2011, **133**, 6825–6831.
13 X. J. Zhu, Y. W. Zhu, S. Murali, M. D. Stoller and R. S. Ruoff, *ACS Nano*, 2011, **5**, 3333–3338.
14 Y. J. Li, W. Gao, L. J. Ci, C. M. Wang and P. M. Ajayan, *Carbon*, 2010, **48**, 1124–1130.

This journal is © The Royal Society of Chemistry 2014

Published on 06 May 2014. Downloaded by Duke University on 25/04/2018 22:20:45.

15 X. C. Dong, W. Huang and P. Chen, *Nanoscale Res. Lett.*, 2011, **6**, 60–65.
16 Y. Chen, X. Zhang, D. C. Zhang, P. Yu and Y. W. Ma, *Carbon*, 2011, **49**, 573–580.
17 K. S. Novoselov, A. K. Geim, S. V. Morozov, D. Jiang, Y. Zhang, S. V. Dubonos, I. V. Grigorieva and A. A. Firsov, *Science*, 2004, **306**, 666–669.
18 F. Schedin, A. K. Geim, S. V. Morozov, E. W. Hill, P. Blake, M. I. Katsnelson and K. S. Novoselov, *Nat. Mater.*, 2007, **6**, 652–655.
19 P. Blake, P. D. Brimicombe, R. R. Nair, T. J. Booth, D. Jiang, F. Schedin, L. A. Ponomarenko, S. V. Morozov, H. F. Gleeson, E. W. Hill, A. K. Geim and K. S. Novoselov, *Nano Lett.*, 2008, **8**, 1704–1708.
20 P. K. Ang, W. Chen, A. T. S. Wee and K. P. Loh, *J. Am. Chem. Soc.*, 2008, **130**, 14392–14393.
21 L. A. Ponomarenko, F. Schedin, M. I. Katsnelson, R. Yang, E. W. Hill, K. S. Novoselov and A. K. Geim, *Science*, 2008, **320**, 356.
22 M. D. Stoller, S. Park, Y. Zhu, J. An and R. S. Ruoff, *Nano Lett.*, 2008, **8**, 3498–3502.
23 Z. F. Wang, J. J. Liu, W. X. Wang, H. R. Chen, Z. H. Liu, Q. K. Yu, H. D. Zeng and L. Y. Sun, *Chem. Commun.*, 2013, **49**, 10835–10837.
24 M. J. McAllister, J. L. Li, D. H. Adamson, H. C. Schniepp, A. A. Abdala, J. Liu, M. H. Alonso, D. L. Milius, R. Car, R. K. Prudhomme and I. A. Aksay, *Chem. Mater.*, 2007, **19**, 4396–4404.
25 Y. W. Zhu, M. D. Stoller, W. W. Cai, A. Velamakanni, R. D. Piner, D. Chen and R. S. Ruoff, *ACS Nano*, 2010, **4**, 1227–1233.
26 G. K. Ramesha and S. Sampath, *J. Phys. Chem. C*, 2009, **113**, 7985–7989.
27 M. Zhou, Y. Wang, Y. Zhai, J. Zhai, W. Ren, F. Wang and S. J. Dong, *Chem.–Eur. J.*, 2009, **15**, 6116–6120.
28 Z. J. Wang, X. Z. Zhou, J. Zhang, F. Boey and H. Zhang, *J. Phys. Chem. C*, 2009, **113**, 14071–14075.
29 X. H. Kang, J. Wang, H. Wu, I. A. Aksay, J. Liu and Y. H. Lin, *B. B.*, 2009, **25**, 901–905.
30 B. Liu, H. T. Lian, J. F. Yin and X. Y. Sun, *Electrochim. Acta*, 2012, **75**, 108–114.
31 H. S. Yin, Q. Ma, Y. L. Zhou, S. Y. Ai and L. S. Zhu, *Electrochim. Acta*, 2010, **55**, 7102–7108.
32 M. Zhang and W. Gorski, *J. Am. Chem. Soc.*, 2005, **127**, 2058–2059.
33 W. S. Hummers and R. E. Offeman, *J. Am. Chem. Soc.*, 1958, **80**, 1339.
34 V. Gau, S. C. Ma, H. Wang, J. Tsukuda, J. Kibler and D. A. Haake, *Methods*, 2005, **37**, 73–83.
35 R. Maskiewicz, D. Sogah and T. C. Bruice, *J. Am. Chem. Soc.*, 1979, **101**, 5347–5354.
36 K. Maeda, T. Kashiwabara and M. Tokuyama, *Bull. Chem. Soc. Jpn.*, 1977, **50**, 473–481.
37 J. H. Chen, Z. Y. Lin and G. N. Chen, *Electrochim. Acta*, 2007, **52**, 4457–4462.
38 Y. G. Sun, H. Cui and X. Q. Lin, *J. Lumin.*, 2001, **92**, 205–211.
39 T. Okajima and T. Ohsaka, *J. Electroanal. Chem.*, 2002, **534**, 181–187.
40 Q. H. Jiang, M. Hakansson, J. Suomi, T. A. Kleme and S. Kulmala, *J. Electroanal. Chem.*, 2006, **591**, 85–92.
41 M. Liu, Y. Hashi, F. Pan, J. Yao, G. Song and J. Lin, *J. Chromatogr. A*, 2006, **1133**, 142–148.
42 G. Gatidou, N. S. Thomaidis, A. S. Stasinakis and T. D. Lekkas, *J. Chromatogr. A*, 2007, **1138**, 32–41.
43 Y. Wen, B. Zhou, Y. Xu, S. Jin and Y. Feng, *J. Chromatogr. A*, 2006, **1133**, 21–28.
44 H. S. Yin, Y. L. Zhou and S. Y. Ai, *J. Electroanal. Chem.*, 2009, **626**, 80–88.
45 M. J. Shi, M. Aung and Y. P. Dong, *Spectrosc. Spectral Anal.*, 2007, **27**, 1945–1950.